Three-Dimensional Numerical Analysis to Determine Unloading Factor in Shallow Tunnels

Arvin Fardipour [a], Mehdi Nodeh [b]*

[a] *Department of Civil Engineering, Islamic Azad University, Rudehen, Tehran, Iran;*
[b] *Institute of sanitary engineering and waste management Leibniz university of Hanover, Hanover, Germany;*
DOI: https://doi.org/10.55248/gengpi.4.923.92503

A B S T R A C T

Tunnel excavation disturbs the initial geostatic stress field, resulting in elastic-plastic deformations around the tunnel. In shallow tunnels, this causes ground movements at the surface and tunnel perimeter. Predicting these changes is vital to minimize harmful effects. Considerable research has focused on developing improved methods to predict tunneling-induced movements. The coefficient of lateral earth pressure (K_0) is a key parameter affecting tunneling movements. Full 3D analysis provides the most realistic assessment of movements, but high computational costs have made 2D analysis standard, except for complex tunnel geometries. To incorporate 3D effects into 2D tunnel analysis, methods like the Stress Reduction approach use an unloading factor (β) to simulate 3D arching. This paper first simulated six 3D models with varying K_0 values. Transverse displacement diagrams were obtained for each model. Next, 2D analysis was performed for the same K_0 values and a range of β from 0.2-0.8. Finally, 3D and 2D transverse displacements were compared to determine the optimal β factor for each model. The models used a circular tunnel with a 100x40x28 block. The Mohr-Coulomb model had E=42 MPa, ν=0.25, c=20 kPa, φ=20°, ψ=0° and varied K_0. An 8m diameter NATM tunnel with 16m cover was modeled. Results showed decreasing β and increasing ground stress relaxation as K_0 increased from <1 to >1. The β factor represents load sharing by the lining, while (1-β) is ground stress relaxation. More ground deformation but lower lining forces occurred with smaller β, while larger β gave less ground but more lining deformation. 3D analysis predicted settlement for K_0<1.2 and heave for K_0>1.2. The optimized β values were 0.7 for K_0=0.5, 0.6 for K_0=1, and 0.5 for K_0=1.2, 1.5, 1.8, 2. This provides guidance for selecting appropriate β factors in comparable tunnel models.

Keywords: Ground movements, Tunnel excavation, PLAXIS, NATM, shallow tunnel, Elastic-plastic deformations, Geostatic stress, Lateral earth pressure, Transverse displacement

1. Introduction

Three-dimensional finite element analysis can provide improved predictions of ground movements caused by underground tunnel excavation. 3D analysis is very comprehensive and can address many research questions. However, the high computational demands of 3D analysis regarding runtimes and memory/processor requirements have made 2D analysis standard practice for most tunnel modeling, except where the excavation geometry is complex (e.g. tunnel intersections or connections to other underground stations) and requires full 3D analysis [1–3]. While 2D analysis can provide good preliminary estimates of tunneling-induced ground movements, 3D analysis is required for more rigorous evaluation, especially when analyzing critical infrastructure where high accuracy is essential [4,5].

Recent studies have employed advanced 3D numerical modeling to investigate various aspects of tunneling-induced ground movements. Do et al. [3] performed 2D and 3D analyses of curved shallow tunnels in Paris, demonstrating the ability of 3D models to capture complex tunnel-soil-structure interaction effects not represented in 2D. Dias and Kastner [4] used 3D analysis to study movements caused by pressurized shield tunneling, validating their model against field data. Do et al. [5] extended their prior 3D modeling to examine the influence of joint patterns on mechanized tunneling through soft ground. A recent study [6] investigated cracking and strength reductions in reinforced concrete corbels caused by construction defects. As the tunneling article notes, proper structural design and construction quality are critical for underground infrastructure. Testing of corbels with flaws like low concrete strength demonstrated significant capacity decreases compared to healthy specimens. This research shows how defects can undermine concrete element performance, with implications for quality control in tunnel lining design. Thorough testing is key for identifying vulnerabilities in reinforced concrete. Franzius et al. [7] investigated the impacts of soil anisotropy and lateral earth pressure coefficient on tunneling-induced ground surface movements through 3D numerical analysis.

Other researchers have applied 3D analysis to study the effects of hydraulic gradients [8], pre-failure soil stiffness [9], and tunnel depth [10] on ground movements due to tunneling. A recent study [11] on concrete recycling demonstrates principles applicable to sustainable underground construction. As the tunneling article notes, large volumes of waste are produced during excavations. Recycling demolition concrete and integrating construction byproducts, as discussed by Shomal Zadeh et al., can reduce environmental impacts of major projects like tunnels. Their work aligns with civil engineering

trends toward eco-friendly infrastructure. Mair [12] provided an overview of innovations in 3D geotechnical modeling and simulation for tunneling applications. Advanced 3D constitutive models incorporating elasto-plastic behavior have been implemented in tunnel analyses to improve modeling of the complex tunnel-soil interaction [13]. Joushideh et al. [14] demonstrated advanced numerical analysis for geotechnical infrastructure like rubble mound breakwaters. By integrating state-of-the-art simulation and investigation tools, failures can be minimized in geotechnical systems like tunnels. This research by Joushideh et al. highlighted the importance of thorough analysis using modern methods for optimal design.

The research by Khodadadi Koodiani et al. [15] demonstrated the use of optimized artificial neural networks and parametric analysis to successfully derive accurate empirical equations for predicting the compressive strength of FRP-confined columns. Their work shows the value of leveraging AI-based techniques like ANNs to improve structural modeling and design.

Sophisticated 3D numerical studies have also examined other aspects of tunnel behavior, including ground movements behind the tunnel face during construction [16], heading stability [17], tunnel lining forces [18], and building response due to tunneling-induced subsidence [19]. Overall, 3D analysis provides a more complete representation of the tunnel excavation process and soil-structure interaction effects compared to 2D approaches. However, 3D modeling requires greater effort and computational resources. Selecting an appropriate 2D or 3D analysis methodology depends on project-specific factors such as tunnel depth, geology, and proximity of vulnerable structures. For critical infrastructure and complex conditions, 3D analysis is recommended to achieve the highest accuracy. Continued advances in numerical modeling software, computing power, and soil constitutive models will further expand the capabilities of 3D tunneling analysis.

2. 3D Tunnel Modeling with PLAXIS 3D TUNNEL

2.1 Model Geometry

The model consists of an 8m diameter tunnel with 16m of cover. The model block dimensions are 100m x 40m x 28m.

To avoid boundary effects, the first 25m of the model employs sequential excavation and installation of tunnel lining. The tunnel section from 25-75m is then analyzed.

2.2 Mesh Generation

15-node triangular elements with a coarse base mesh are used. Local mesh refinement is applied at key areas like the ground surface, tunnel interior, and vertical section above the tunnel (crown). Symmetry reduces computations by modeling just half the tunnel (Figure 1).
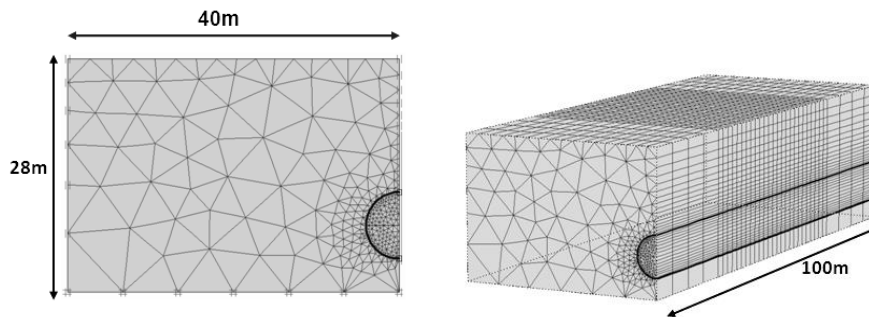

Fig. 1 - Schematic representation of two-dimensional meshing and three-dimensional models

2.3 Geotechnical Properties

The model uses a homogeneous sandy clay soil. The Mohr-Coulomb model provides more realistic behavior than linear-elasticity, and its parameters are readily obtained. A drained analysis is performed. Table 1 summarizes the soil properties.

Table 1 - Soil Mechanical Properties

Parameter	unit	Value
γ	(KN/m^3)	19
E	(KN/m^2)	42×10^3
ν	-	0/25
C	(KN/m^2)	20
$\acute{\phi}$	-	20
ψ	-	0

3. 3D NATM Tunneling Methodology

The 3D block consists of sequential slices, each 2m long, representing one excavation round. In step i-1, the soil is removed from slice 1. In step i, slice 2 is excavated and lining installed in slice 1. This continues sequentially for each slice (Figure 2). This incremental approach simulates the NATM process.

As shown in the 3D model, soil elements are removed from slice X to represent one excavation round, with lining installed in slice X during the next step. Delaying lining installation allows the ground to relieve stresses, which is fundamental to NATM tunneling.

The tunnel profile is circular. The lining is elastic with no self-weight. Excavation occurs in upper and lower halves. Lining properties are given in Table 2.

Table 2 – Lining Mechanical Properties

Parameter	unit	Value
AE	KN/m	6×10^6
EI	KN.m^2/m	$4/5\times10^4$
D	m	$0/3$
ν	-	0
W	KN/m/m	0
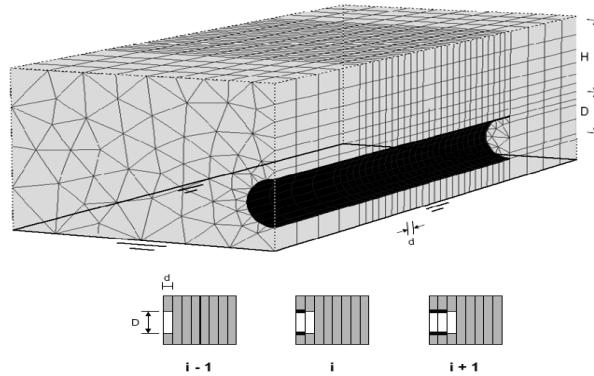
Figure 2 – Step-by-step NATM tunneling sequence

4. 2D NATM Analysis Methodology

To incorporate 3D effects in 2D NATM analysis, methods like the following are used:

- Core Support (α)

- Lining Reduction (δ)

- Stress Reduction (β)

The Stress Reduction method is the most popular approach. It represents stress relief due to delayed lining installation and appropriate load sharing between ground and lining.

The two analysis phases are:

1. Apply in situ stresses and activate reduced pressure P0(1-β) to simulate tunnel excavation without support.

2. Install tunnel lining and distribute pressure P0β to lining and ground.

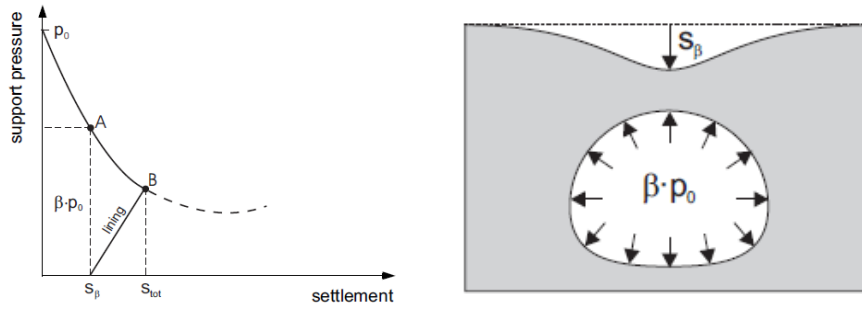Figures 3 and 4 illustrate the stress reduction method in relation to the ground response curve.

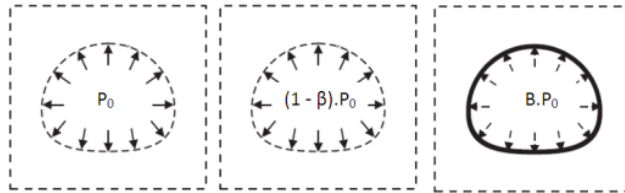Fig. 3 - Ground response curve for stress reduction

Figure 4 - Stress reduction method calculation phases

β is the stress reduction factor, also called the unloading factor, representing the percentage of initial ground stress carried by the installed lining.

5. 2D Tunnel Modeling with PLAXIS 2D

5.1 Geometry, Mesh and Properties

The 2D dimensions match the 3D model cross-section: 40m wide x 28m high (Figure 5). 15-noded triangles and local mesh refinement are again used. Geotechnical properties match the 3D analysis.
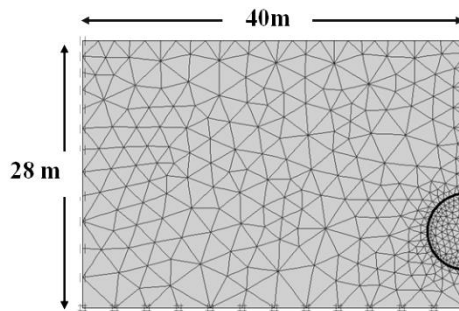
Figure 5- Two-dimensional analysis mesh schematic

6. 3D Analysis Results

Figure 6 shows transverse displacement curves from the 3D analyses for varying K0.

The profiles indicate a transition from shallow settlement to increasing heave as K0 increases from <1 to >1. Table 3 summarizes the 3D transverse displacements.

Table 3 – 3D Transverse Displacements

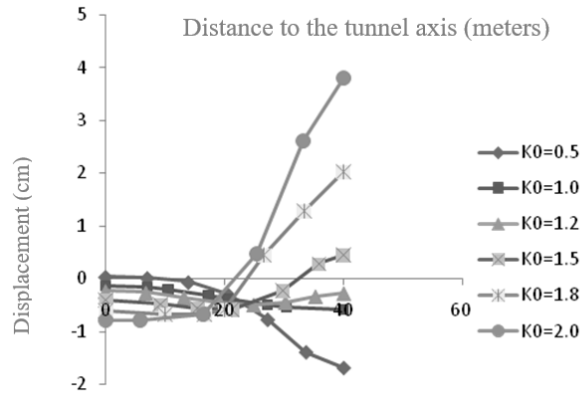| Maximum transverse displacement (cm)	Coefficient of lateral pressure of the soil
-1 /7	0/5
-0 /59	1
-0/5	1/2
+0 /45	1/5
+2 /02	1/8
+3 /8	2

Figure 6- 3D displacement curves for different K0 values

7. 2D Analysis and Comparison to 3D Results

Based on tunneling measurements, Swoboda & Laabmayr (1986) proposed β ranges of 0.2-0.8. The same range is analyzed here.

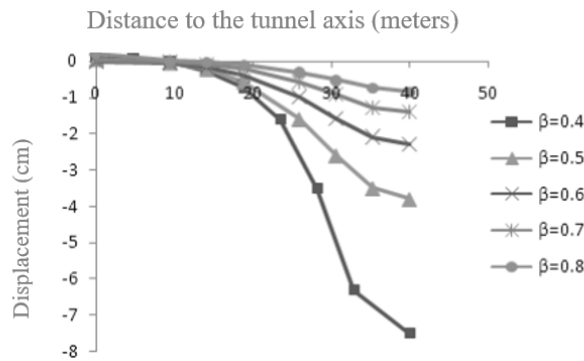Figure 7 shows the 2D displacement curves for K0=0.5. Analysis failed to converge for β=0.2 and 0.3.

Figure 7- 2D transverse displacement curves with different values of β, K0=0.5

For K0=0.5, the 2D profile for β=0.7 closely matches the 3D result. The 3D and 2D maximum settlements are -7.1cm and -4.1cm respectively (Figure 8).
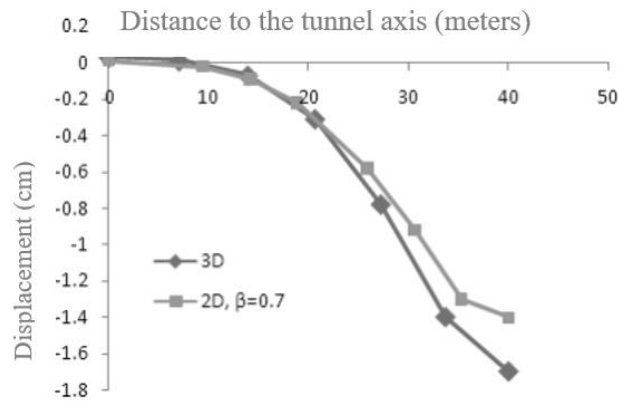
Figure 8 - Comparison of 2D and three-dimensional transverse displacement curves, K0=0.5

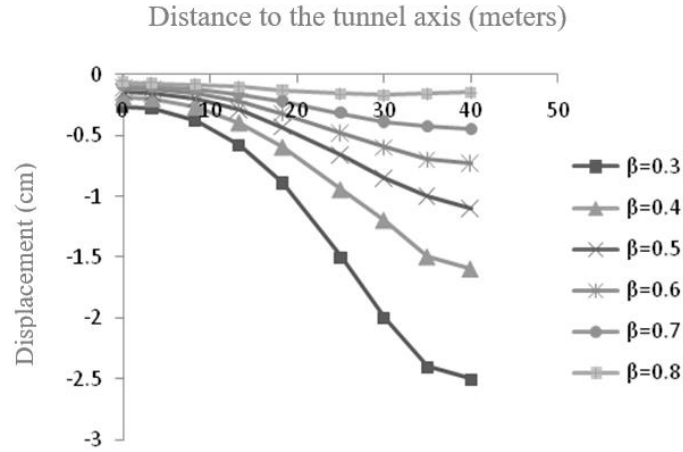Figure 9 presents the K0=1 displacement curves. β=0.2 again failed to converge.

Figure 9 - 2D transverse displacement curves with different values of β, K0=1

For K0=1, the 2D β=0.6 curve best fits the 3D profile, with respective settlements of -59.0cm and -73.0cm (Figure 10).

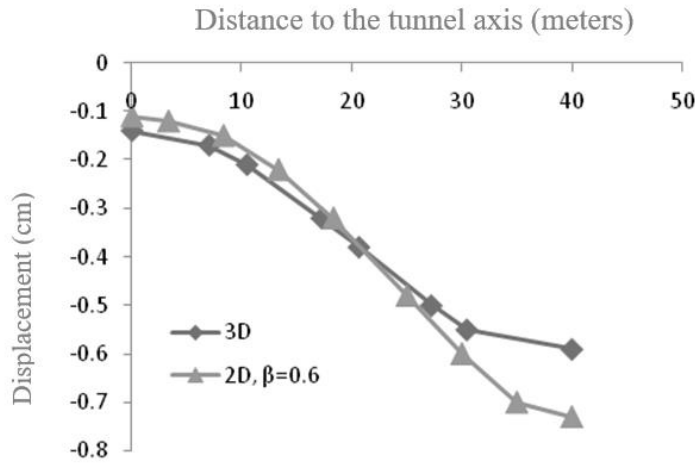**Figure 10- Comparison of 2D and three-dimensional transverse displacement curve, K0 =1**

The K0=1.2 results are shown in Figure 11. The β=0.5 2D curve most closely resembles the 3D case, although the maximum settlements are -77.0cm and -28.0cm respectively (Figure 12).
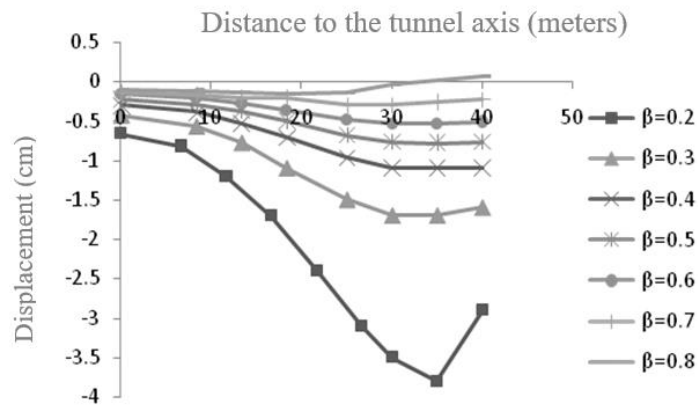

Figure 11- 2D transverse displacement curves with different values of β, K0=1.2
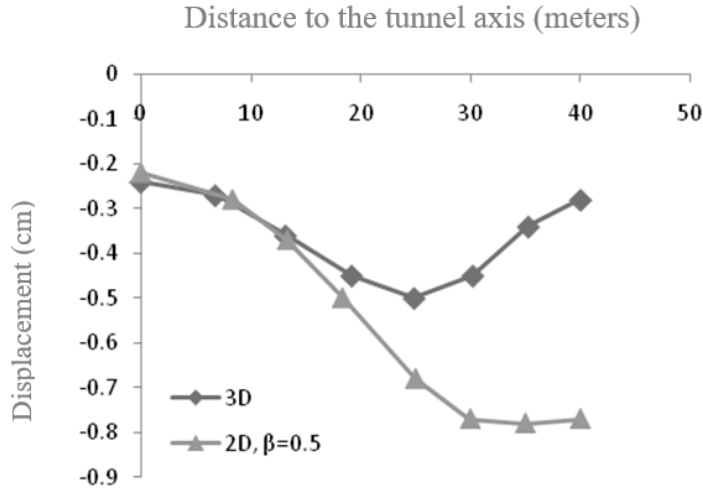
Figure 12- Comparison of 2D and 3D transverse displacement curve, K0=1.2

Figure 13 provides the K0=1.5 outcomes. Here, the 3D profile shows 45.0cm heave, while the β=0.5 2D curve indicates -35.0cm settlement. This 2D case best matches the 3D heave behavior (Figure 14).
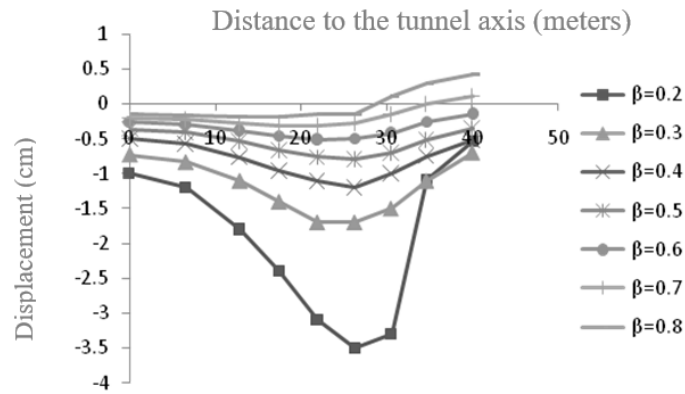

Figure 13- 2D transverse displacement curves with different values of β, K0=1.5

For K0=1.8, a β value of 0.5 was again obtained, with 2D and 3D heaves of 45.0cm and 102.2cm respectively (Figures 15 and 16).
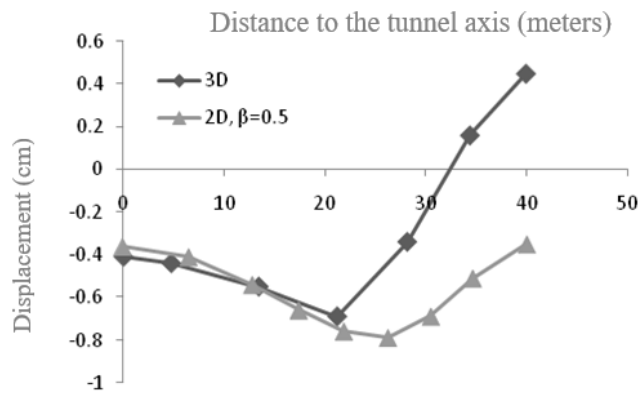

Figure 14- Comparison of 2D and 3D transverse displacement curve, K0 = 1.5
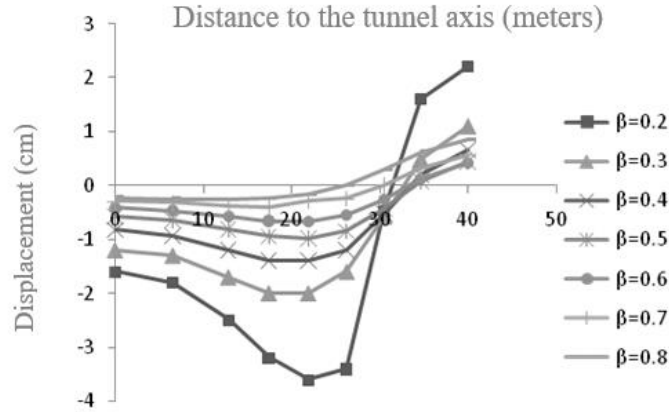
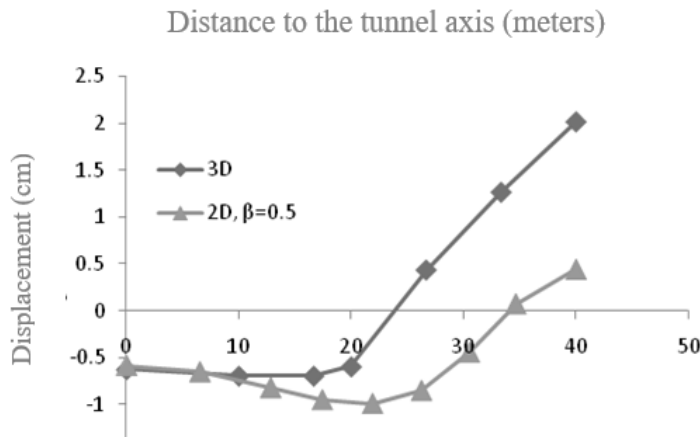**Figure 15- 2D transverse displacement curves with different values of β, K0=1.8**

Figure 16- Comparison of 2D and 3D transverse displacement curves, K0=1.8

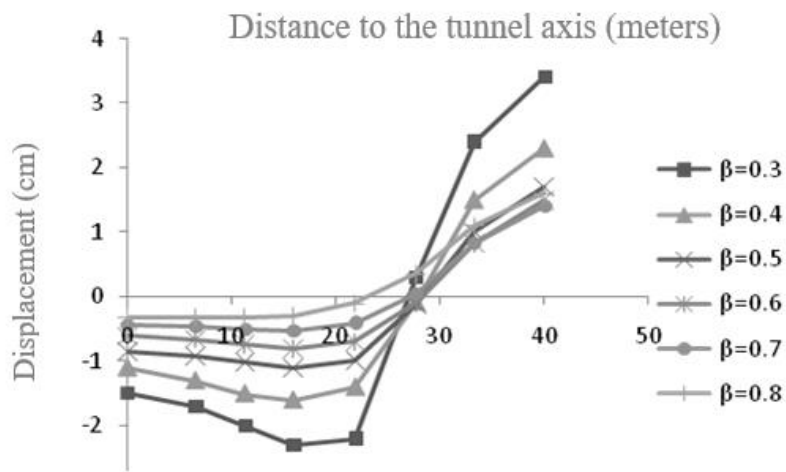Finally, for K0=2 the optimized β was 0.5. Respective 2D and 3D heaves were 7.1cm and 8.3cm (Figures 17 and 18).

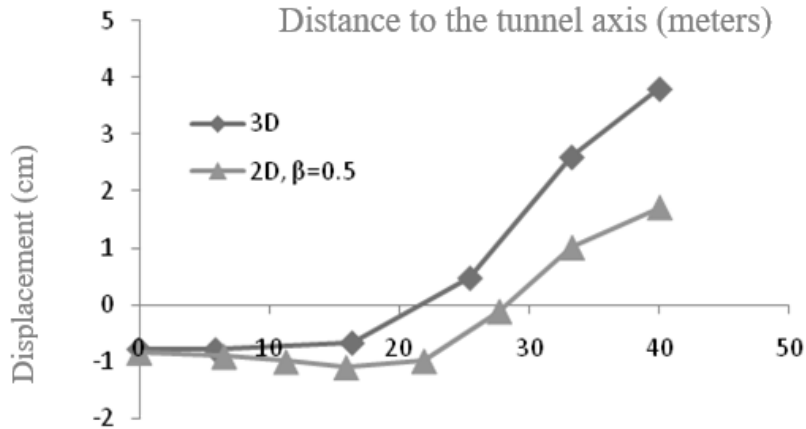**Figure 17- 2D transverse displacement curves with different values of β, K0=2**

Figure 18- Comparison of 2D and 3D transverse displacement curves, K0=2

8. Conclusions

The β factor depends on cross-section, excavation steps, material properties and construction methods, so accurate determination is difficult. However, β ranges can be estimated from experience, field measurements, theoretical assumptions and 2D vs 3D comparative analysis.

β values will not apply uniformly to all tunnels due to variations in geometry, boundary conditions and analysis methods. The β values found here apply for homogeneous sandy clay with Mohr-Coulomb behavior, shallow NATM tunnels, 2m rounds and circular profiles. They provide reasonable estimates for comparable tunnel models.

Tunnel excavation unloads the ground, relaxing stresses. For K0=0.5, 1 and >1, approximate ground stress reliefs of 30%, 40% and 50% respectively were observed. Increasing K0 from <1 to >1 leads to greater stress relaxation. As the lateral earth pressure coefficient K0 increases, the ground stress relief also increases due to the unloading caused by tunnel excavation. Based on the 3D numerical analyses conducted here, the degree of ground stress relief was approximately 30%, 40%, and 50% for K0 values of 0.5, 1, and greater than 1, respectively.

As ground stresses reduce, lower loads are transferred to the lining. Since β represents lining load share, it decreases with increasing K0. The degree of ground stress relief has a direct effect on the loads carried by the tunnel lining. With greater stress relief in the ground, lower loads are transferred to the lining after excavation. Because the β factor represents the proportion of the overburden load carried by the lining, its value decreases as the ground stress relief increases with higher K0.

Lower β reduces lining loads and structural forces. With a lower β factor, the loads on the tunnel lining are reduced, which consequently reduces the internal forces (e.g., bending moments and thrusts) in the lining structure.

With greater ground stress relief, deformations increase in the ground but decrease in the lining. Smaller β gives larger ground and smaller lining deformations, while higher β does the opposite. As K0 and ground stress relief increase, the deformations in the ground around the tunnel become larger due to the lower remnant stresses. However, the deformations in the lining decrease as its load share is reduced with lower β. Therefore, a lower β leads to larger ground movements but smaller lining deformations, while a higher β produces smaller ground but larger lining movements.

The 3D analyses showed a transition from settlement to heave as K0 increased past 1.2 at the tunnel centerline. Based on the results of the comprehensive 3D numerical simulations, the vertical displacements at the ground surface directly above the tunnel centerline transitioned from settlement to heave as the K0 value increased beyond approximately 1.2. This demonstrates the sensitivity of ground surface movements to the lateral earth pressure coefficient.

The stability of a tunnel heading is dependent on the state of stresses around the face during excavation. In particular, the distribution of shear stresses and presence of yield zones in the ground determine heading stability.

Sophisticated 3D constitutive models are required to accurately capture the nonlinear and anisotropic behavior of soils and rocks during tunneling. Advanced models such as Hoek-Brown and Hou/Lu that incorporate plasticity and failure provide realistically simulated ground-tunnel interaction.

Building damage risk assessment for tunneling projects requires realistic 3D simulation of ground movements as well as advanced structural modeling of buildings. Coupling sophisticated geotechnical and structural analysis enables reliable prediction of tunneling impacts on buildings.

References

1. Lee, K.; Rowe, R.K.; Lo, K. Subsidence Owing to Tunnelling. I. Estimating the Gap Parameter. Canadian geotechnical journal 1992, 29, 929–940.

2. Möller, S.; Vermeer, P. On Numerical Simulation of Tunnel Installation. Tunnelling and Underground Space Technology 2008, 23, 461–475.

3. Do, N.-A.; Dias, D.; Oreste, P. 3D Numerical Investigation on the Interaction between Mechanized Twin Tunnels in Soft Ground. Environmental Earth Sciences 2015, 73, 2101–2113.

4. Dias, D.; Kastner, R. Movements Caused by the Excavation of Tunnels Using Face Pressurized Shields—Analysis of Monitoring and Numerical Modeling Results. Engineering Geology 2013, 152, 17–25.

5. Do, N.-A.; Dias, D.; Oreste, P.; Djeran-Maigre, I. Three-Dimensional Numerical Simulation of a Mechanized Twin Tunnels in Soft Ground. Tunnelling and Underground Space Technology 2014, 42, 40–51.

6. Shabbir, F.; Bahrami, A.; Ahmad, I.; Shakouri Mahmoudabadi, N.; Iqbal, M.; Ahmad, A.; Özkılıç, Y.O. Experimental and Numerical Investigation of Construction Defects in Reinforced Concrete Corbels. Buildings 2023, 13, 2247, doi:10.3390/buildings13092247.

7. Franzius, J.; Potts, D.; Burland, J. The Influence of Soil Anisotropy and K_0 on Ground Surface Movements Resulting from Tunnel Excavation. Géotechnique 2005, 55, 189–199.

8. Neaupane, K.M.; Adhikari, N. Prediction of Tunneling-Induced Ground Movement with the Multi-Layer Perceptron. Tunnelling and underground space technology 2006, 21, 151–159.

9. Addenbrooke, T.; Potts, D.; Puzrin, A. The Influence of Pre-Failure Soil Stiffness on the Numerical Analysis of Tunnel Construction. Géotechnique 1997, 47, 693–712.

10. Hunt, D. Predicting the Ground Movements above Twin Tunnels Constructed in London Clay. 2005.

11. Shomal Zadeh, S.; Joushideh, N.; Bahrami, B. A Review on Concrete Recycling. World Journal of Advanced Research and Reviews 2023, 19, 784–793, doi:10.30574/wjarr.2023.19.2.1631.

12. Mair, R.J. Tunnelling and Geotechnics: New Horizons. Géotechnique 2008, 58, 695–736, doi:10.1680/geot.2008.58.9.695.

13. Carranza-Torres, C.; Fairhurst, C. The Elasto-Plastic Response of Underground Excavations in Rock Masses That Satisfy the Hoek–Brown Failure Criterion. International Journal of Rock Mechanics and Mining Sciences 1999, 36, 777–809.

14. Joushideh, N.; Shomal Zadeh, S.; Bahrami, B.; Shakouri Mahmoudabadi, N. Pseudo-Static Slope Stability Analysis and Numerical Settlement Assessment of Rubble Mound Breakwater under Hydrodynamic Conditions. World Journal of Advanced Research and Reviews 2023, 19, 273–287, doi:10.30574/wjarr.2023.19.2.1542.

15. Khodadadi Koodiani, H.; Erfanian, N.; Majlesi, A.; Hosseinzadeh, A.; Jafari, E.; Shahin, M.; Matamoros, A. Calibrating Equations to Predict the Compressive Strength of FRP-Confined Columns Using Optimized Neural Network Model. Structures 2023, 56, 105060, doi:10.1016/j.istruc.2023.105060.

16. Panet, M.; Guenot, A. Analysis of Convergence behind the Face of a Tunnel. 1982.

17. Vermeer, P.A.; Ruse, N.; Marcher, T. Tunnel Heading Stability in Drained Ground. Felsbau 2002, 20, 8–18.

18. Möller, S.C. Tunnel Induced Settlements and Structural Forces in Linings; Univ. Stuttgart, Inst. f. Geotechnik Stuttgart, Germany, 2006; ISBN 3-921837-54-5.

19. Franzius, J. Behavior of Buildings Due to Tunnel Induced Subsidence. Ms. c. 2003.